BNL-96182-2011-CP

Compact CdZnTe-based gamma camera for prostate cancer imaging

Y. Cui, T. Lall, B. Tsui, J. Yu, G. Mahler, A. Bolotnikov, P. Vaska, G. De Geronimo, P. O'Connor, G. Meinken, J. Joyal, J. Barrett, G. Camarda, A. Hossain, K.H. Kim, G. Yang, M. Pomper, S. Cho, K. Weisman, Y. Seo, J. Babich, N. LaFrance, and R.B. James

Presented at the 2011 IEEE Nuclear Science Symposium and Medical Imaging Conference (2011 NSS/MIC)
Valencia, Spain
October 23-29, 2011

August 2011

Nonproliferation and National Security Department

Brookhaven National Laboratory

U.S. Department of Energy
Office of Science, National Nuclear Security Administration

DISCLAIMER

Compact CdZnTe-based gamma camera for prostate cancer imaging

Yonggang Cui[a*], Terry Lall[b], Benjamin Tsui[c], Jianhua Yu[c], George Mahler[a], Aleksey Bolotnikov[a], Paul Vaska[a], Gianluigi De Geronimo[a], Paul O'Connor[a], George Meinken[a], John Joyal[f], John Barrett[f], Giuseppe Camarda[a], Anwar Hossain[a], Ki Hyun Kim[a], Ge Yang[a], Marty Pomper[c], Steve Cho[c], Ken Weisman[d], Youngho Seo[e], John Babich[f], Norman LaFrance[f], and Ralph B. James[a]

[a] Brookhaven National Laboratory, Upton, NY 11973, USA

[b] Hybridyne Imaging Technologies, Inc., Toronto, ON M2N 6K1, Canada

[c] Johns Hopkins University, Baltimore, MD 21205, USA

[d] Midstate Hospital, Meriden, CT 06451, USA

[e] University of California at San Francisco, San Francisco, CA 94107, USA

[f] Molecular Insight Pharmaceuticals, Cambridge, MA 02142, USA

ABSTRACT

In this paper, we discuss the design of a compact gamma camera for high-resolution prostate cancer imaging using Cadmium Zinc Telluride (CdZnTe or CZT) radiation detectors. Prostate cancer is a common disease in men. Nowadays, a blood test measuring the level of prostate specific antigen (PSA) is widely used for screening for the disease in males over 50, followed by (ultrasound) imaging-guided biopsy. However, PSA tests have a high false-positive rate and ultrasound-guided biopsy has a high likelihood of missing small cancerous tissues. Commercial methods of nuclear medical imaging, e.g. PET and SPECT, can functionally image the organs, and potentially find cancer tissues at early stages, but their applications in diagnosing prostate cancer has been limited by the smallness of the prostate gland and the long working distance between the organ and the detectors comprising these imaging systems.

CZT is a semiconductor material with wide band-gap and relatively high electron mobility, and thus can operate at room temperature without additional cooling. CZT detectors are photon-electron direct-conversion devices, thus offering high energy-resolution in detecting gamma rays, enabling energy-resolved imaging, and reducing the background of Compton-scattering events. In addition, CZT material has high stopping power for gamma rays; for medical imaging, a few-mm-thick CZT material provides adequate detection efficiency for many SPECT radiotracers. Because of these advantages, CZT detectors are becoming popular for several SPECT medical-imaging applications.

Most recently, we designed a compact gamma camera using CZT detectors coupled to an application-specific-integrated-circuit (ASIC). This camera functions as a trans-rectal probe to image the prostate gland from a distance of only 1-5 cm, thus offering higher detection efficiency and higher spatial resolution. Hence, it potentially can detect prostate cancers at their early stages. The performance tests of this camera have been completed. The results show better than 6-mm resolution at a distance of 1 cm. Details of the test results are discussed in this paper.

Keywords: CdZnTe, Radiation Detectors, Prostate Cancer, Nuclear Medical Imaging, Gamma Camera

1. INTRODUCTION

Prostate cancer is one of the most common cancers in the male population. According to the American Cancer Society, about 1 in 6 men will be diagnosed with prostate cancer during his lifetime; in 2010, about 217,730 new cases were diagnosed, and about 32,050 men died of the disease [1]. Furthermore, prostate cancer is the second leading course of cancer death in America. Early detection of the prostate cancer plays an important role in the effectiveness of its treatment. A blood test of the level of the prostate specific antigen (PSA) often is used as the initial screening marker in this process. However, the PSA tests have limitations, as it is not cancer-specific but tissue-specific [2]. An elevated PSA level normally triggers further examinations, e.g., a digital rectal exam to study abnormalities in the size and shape of the gland, followed by (ultrasound) image-guided biopsy to verify the presence of cancer. During the biopsy

* ycui@bnl.gov; phone 1 631 344-5351; fax 1 631 344-876; www.bnl.gov

procedure, the prostate is divided into several regions, and tissue samples are removed randomly from each for examination. Small cancerous tissues are likely to be missed in this painful procedure.

Nuclear-medical imaging affords accurate information about anatomic- and metabolic-processes, increasingly playing an important role in diagnosing cancers. Such imaging techniques include computed tomography (CT), magnetic resonance imaging (MRI), positron emission tomography (PET), and single photon-emission computed tomography (SPECT). However, several factors limit the applications of commercial systems in clinical studies. CT has poor contrast resolution for soft tissues and cannot distinguish the boundary between cancerous- and normal-tissue [3]. MRI may not always differentiate cancer tissue and edema fluid [5], and some regions of prostate gland have low intensity signals on MR images. Functional MRI systems are being developed, but the guidelines for using them have not been established [3]. PET and SPECT can image the distribution of radioactive tracers introduced into the patient's body, and monitor the metabolism of specific organs. In principle, PET and SPECT imaging systems can detect small tumors at early stages. However, most commercial systems are bulky, and they use scintillation detectors to detect gamma-ray photons emitted from the tracers. During medical examinations, the detectors of the imaging system are far away (e.g., 50+ cm) from the imaged organs. At such a long working distance, the efficiency of detection (gamma-ray photon) and spatial resolution are low. The examination process can take several 10's of minutes. In addition, these systems are very expensive.

Because of these limitations in current imaging systems, patients and physicians are demanding new techniques to improve the process of diagnosing prostate cancer. One possibility is based on nuclear medical-imaging technology that is inexpensive and can provide high spatial- and detection-efficiency. Recently, we developed a compact gamma camera (ProxiScan™) using Cadmium Zinc Telluride (CdZnTe or CZT) radiation detectors. CZT is a semiconductor material with wide band-gap and relatively high electron mobility, and thus it can operate at room temperature without additional cooling. The CZT detector is a photon-electron direct-conversion device, thus potentially offering higher energy-resolution in gamma-ray detection; it enables energy-resolved imaging, allowing the subtraction of the background due Compton scattering-events. In addition, CZT material has high stopping power for gamma rays. For medical imaging, a few-mm-thick CZT material affords sufficient detection efficiency. Because of these advantages, CZT detectors are becoming popular for several SPECT medical imaging applications. In this project, we developed a compact gamma camera, ProxiScan™, for imaging prostate cancer. Basically, we integrated the CZT detectors, together with application-specific-integrated-circuits (ASICs) for signal readout into a stainless-steel sheath with an outer diameter of 25 mm. This camera works as a trans-rectal probe to image the prostate gland at a short distance of 1-5 cm, so offering high detection- efficiency and high spatial-resolution. In this paper, we discuss the detailed design of the camera and present the results from performance tests and preclinical animal tests.

2. SYSTEM DESIGN

2.1 Detector development

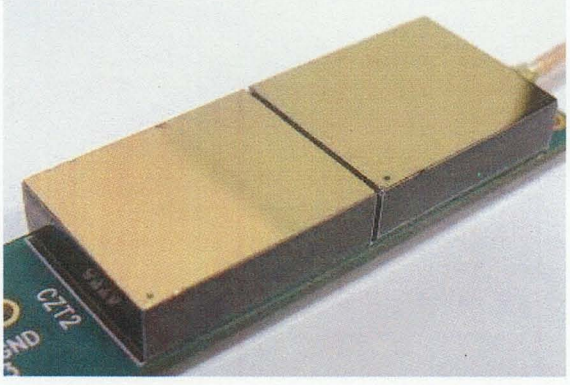

Figure 1. Pixilated CZT detectors employed in the ProxScan™ gamma camera system.

The detectors for the gamma camera are pixilated CZT detectors. We optimized the detectors' thickness for high detection-efficiency and to fit within limited space inside the probe. Based on our calculations, we selected 5-mm-thick

CZT crystals that ensure 76% detection efficiency for Tc-99m gamma-rays at 140.5 keV. The pixel pitch of the detectors was 2.46 mm in the first prototype system. Each system used two detectors, and each detector had a 6x8 pixel array.

2.2 Readout ASIC

A multiple energy window ASIC (MWASIC) [6] developed at Brookhaven National Laboratory (BNL) was employed in the gamma camera to read out signals from the CZT detectors. Each ASIC has 64 readout channels, and each of them has a dedicated charge-sensitive amplifier (CSA), shaping circuits, discriminators, and digital counters for each energy window (Figure 2). The low-noise CSA was optimized for CZT pixilated detectors. The shaping circuits have a 9th-order semi-Gaussian architecture to ensure a high counting rate [6].

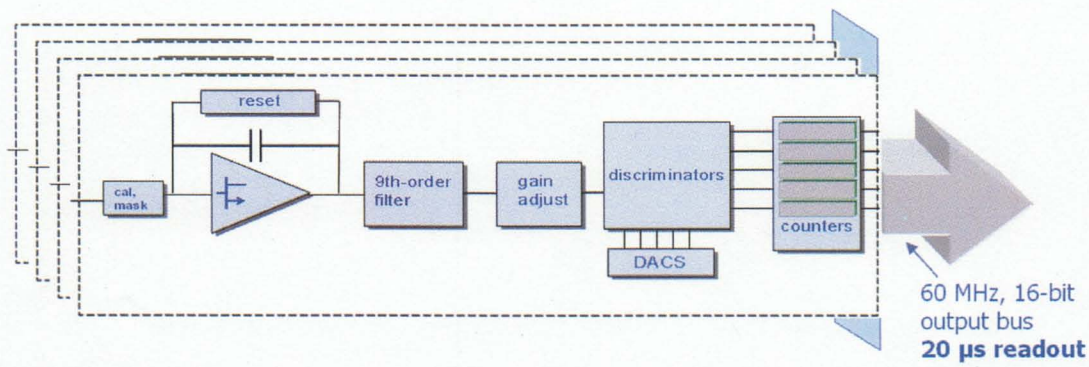

Figure 2. Block diagram of multiple energy window ASIC (MWASIC) [6].

2.3 System design

Figure 3 is a block diagram of the gamma camera system. The CZT detectors and the appropriate ASICs are attached together on two sides of the PCB board. A Cypress microcontroller, FX2LP, controls the ASIC and read-out data. To ensure the highly compact design, we also integrated power-management circuits, low-voltage regulation, and high-voltage generation, into the probe. Externally, we provided a single DC power supply, and a USB port for communication with the computer. Figure 4 is a photograph of the fully integrated gamma-camera.

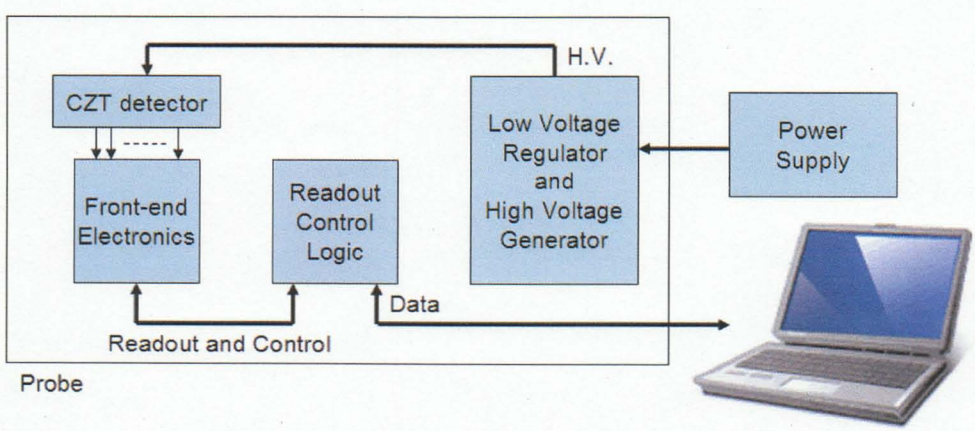

Figure 3. Block diagram of ProxScan™ gamma camera. The compact design has gamma-ray detectors, readout electronics, control logic and voltage generator integrated into a hand-held probe.

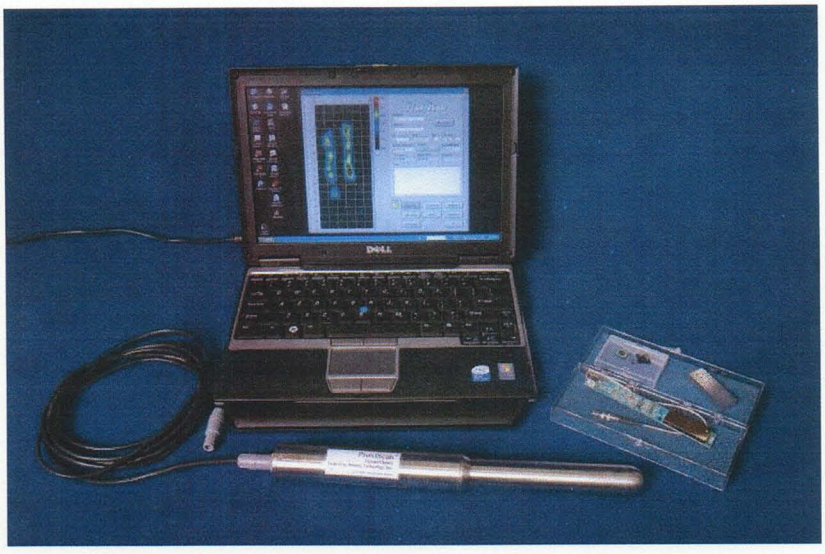

Figure 4. Photo of ProxScan™ compact gamma camera.

3. PERFORMANCE CHARACTERIZATION

The performance of the camera has been tested in the lab; some of the important features are discussed below.

3.1 Energy resolution

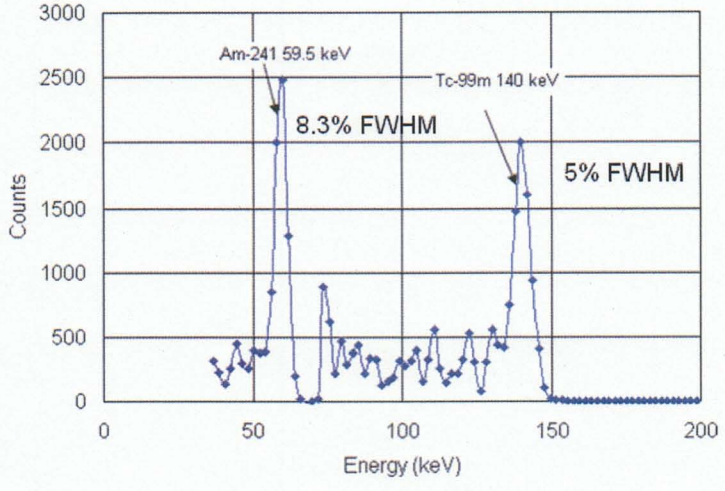

Figure 5. Spectra of Am-241 and Tc-99m isotopes coilected by ProxiScan™ gamma camera. Good energy resolution of 5% (FWHM) was obtained for the Tc-99m 140.5-keV energy line.

The energy resolution of the camera was measured by exposing the camera to different sealed sources (Am-241 and Tc-99m) and scanning the threshold of a specific energy-window. Figure 5 shows the findings exhibiting a 5% full-width-half-maximum (FWHM) for the Tc-99m 140.5-keV line. The result is better than scintillator detectors, which normally are used in nuclear-medical imaging systems (FWHM is ~15% for many commonly used scintillators).

3.2 Energy linearity

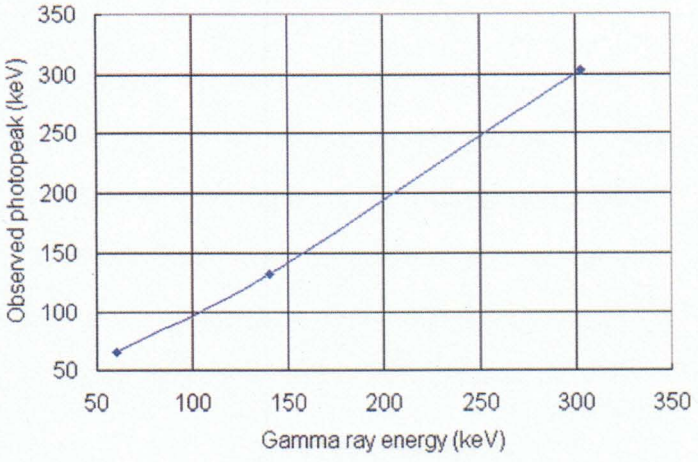

Figure 6. Energy linearity of ProxiScan™ gamma camera. The results demonstrated good linearity from 59.5 to 303 keV covering the energies of gamma-rays emitted by Tc-99m, I-123 and In-111 tracers, which are mostly used as radiopharmaceuticals for SPECT.

The energy linearity of the camera was tested by measuring peak positions of several sealed sources including Am-241 (59.5 keV), Tc-99m (140.5 keV), and Ba-133 (303 keV). As shown in Figure 6, the camera has good linearity in the energy range up to 303 keV, covering the photon peaks of Tc-99m, I-123 and In-111, which are three frequently used radioisotopes used today for nuclear medical imaging.

3.3 Counting rate

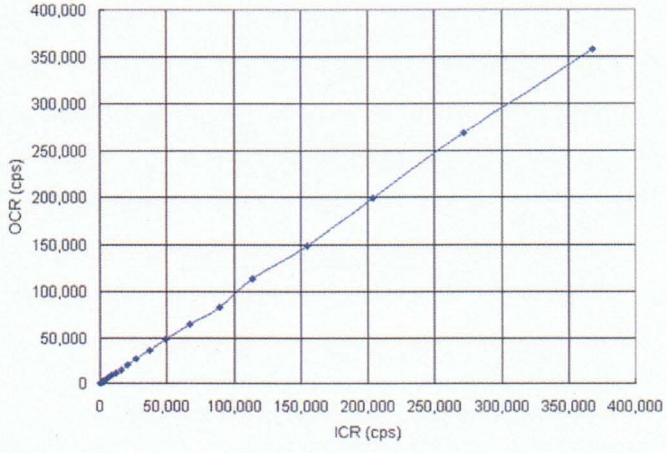

Figure 7. Counting rate characteristic of the gamma camera.

The counting rate characteristic was tested using a procedure similar to that described in the NEMA standard [8]. Because the readout electronics and the MWASIC was optimized for a low-noise, high rate application, it ensured a good counting rate, as shown in Figure 7.

4. IMAGING TESTS

In order to verify the imaging performance of the gamma camera, several tests were undertaken, including a spatial-resolution test, a contrast test, and one for the camera's response to shaped phantoms. We report the results in the following section.

4.1 Spatial resolution

For the spatial-resolution test we used a Tc-99m point-source with a diameter of 0.3 mm and an activity of 6.6 μCi at the time of the experiment. The source was placed above the camera's detector plane, and at different distances from it (d), viz., 0, 13-, 23-, 43-, 63- and 83-mm. At each position, we acquired the point-spread function (PSF) for a 2-min collection time. Figure 8 illustrates the raw images. The green grid in the images indicates the size of the pixel, 2.46x2.46 mm^2. To calculate the spatial resolution, we fit a Gaussian function into each image and extracted the FWHM value. We repeated this calculation for images of d = 0, 13, 23, and 43 mm, covering the distance range from the camera to the prostate gland in patients. The results show the camera has 5.7 mm resolution at a distance of 23 mm, which approximates the distance from the camera to the center of the prostate gland.

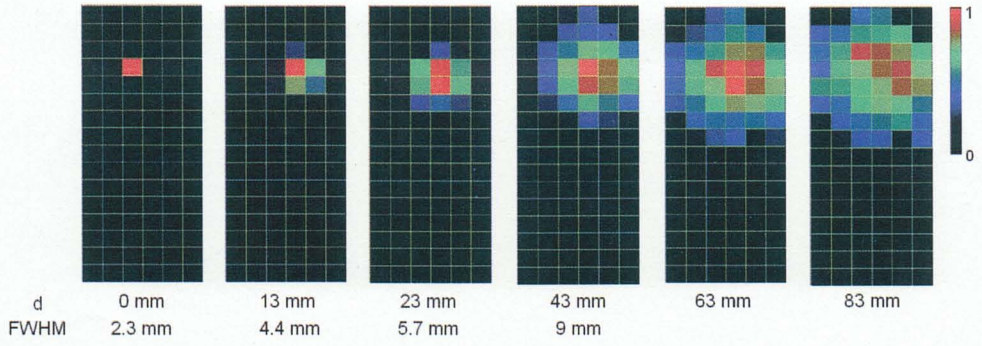

Figure 8. Response of the ProxiScan™ gamma camera to a point source at different distances (d). The green grid indicates the size of the pixels. The spatial resolution was calculated by fitting a Gaussian distribution into each image.

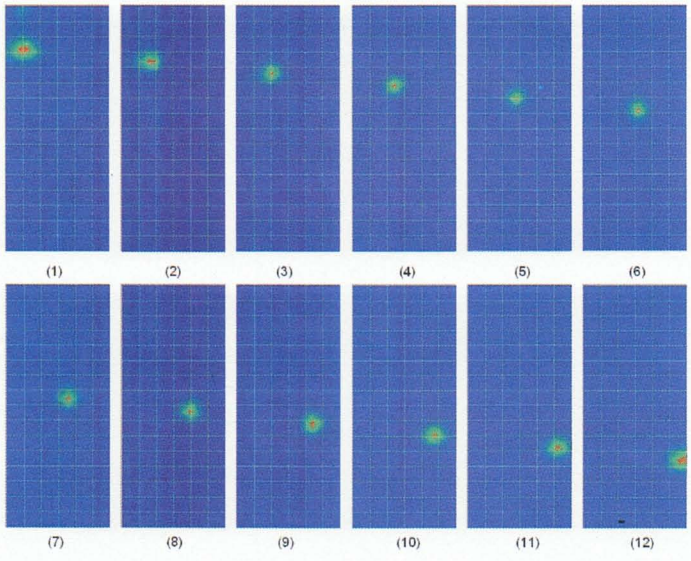

Figure 9. Images after processing with an ML-EM algorithm. The images show the movement of a point source with a step of 1 mm to the left and 2 mm to the bottom of the field-of-view. The centroid in each image was estimated.

4.2 Images after software-image processing

For image processing, we implemented a maximum likelihood estimation expectation maximization (ML-EM) algorithm. To test it, we moved one sealed Co-57 source within the field-of-view (FOV) of the camera with a step of 1 mm to the right and 2 mm down to the bottom. A series of images was taken during this process as shown in Figure 9. As the images reveal, the ML-EM algorithm could estimate the centroid of the sealed source very accurately. This feature is very important in clinical applications, potentially enabling physicians to undertake image-guided biopsy with ~~of~~ ProxiScan™. During the procedure, the physicians want to take bio-samples from the center of the cancerous tissues.

4.3 Shaped source test

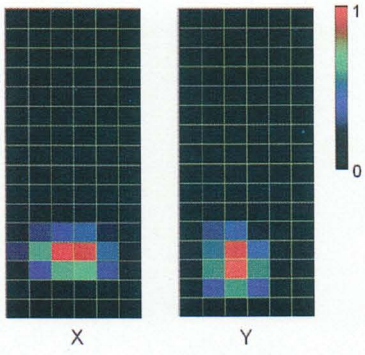

Figure 10. Response of ProxiScan™ gamma camera to a shaped source. The cylindrical phantom for this test was 7.3 mm in length and 3.6 mm in diameter. It was placed at two different orientations, horizontally (X) and vertically (Y). In both cases, the shape of the phantom was resolved.

For this test, we used a cylindrical phantom (Tc-99m), 7.3 mm in length and 3.6 mm in diameter. Its activity was 22 μCi at the time of the experiment. The phantom was placed at two different positions during the testing: X-position, wherein the axis of the phantom was parallel to the shorter edge of the FOV of the camera, and in the Y-position, where the axis was parallel to the longer edge of the FOV. In both cases, the phantom was placed 13 mm above the camera. As shown in Figure 10, the shape of the phantom was resolved in both orientations.

4.4 Contrast test

In addition to the dependence of the image quality on the system performance, it also depends on the performance of the radiopharmaceutical used in the examination. The purpose of the contrast test was to establish the lower boundary of activity ratio of the hot spot (cancerous tissue) to the background (normal tissue and surrounding organs) that the camera can detect. For this test, we used two shaped sources, one flood source and one point source. The flood source is a 10-mm tall acrylic plate container with a 3-mm thick active region. The container was filled with 230 μCi/ml of Tc-99m for the experiment. The point source is a sphere container with a 3.9-mm diameter; it was filled with Tc-99m of different concentrations to obtain ratios of 8:1, 4:1 and 2:1 radioactivity to the flood source. For 2:1 ratio, we tested two different source positions in the test: For position A, the sphere source is above the flood source; and for position B, the sphere is underneath the flood source (Figure 11). Due to photon scattering in the acrylic material, position A has lower contrast than position B. For the 8:1 and 4:1 ratios, only position A was used. For each setup, we collected images for 2 minutes. Figure 12 shows the images. In addition to the high contrast images for the 8:1 and 4:1 configurations, the camera detected the hot spot in a low contrast (2:1) as well. Even in the 2:1 position-A configuration (lower contrast than 2:1), the hot spot still was visible because of the camera's high sensitivity.

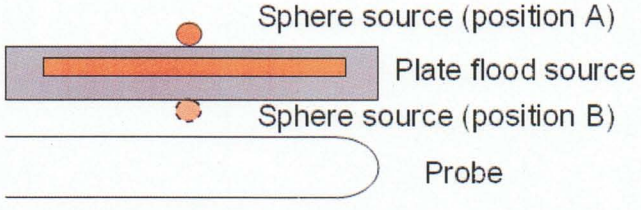

Figure 11. Experimental setup for contrast tests. The flood source was in a 10-mm thick acrylic container with 3-mm thick active volume. The sphere source had a diameter of 3.9 mm. The activity ratio of the sphere source to the flood source was set as 2:1, 4:1, and 8:1. Two different positions of the sphere source, A and B, were tested for the 2:1 ratio. For other ratios, only position A was used.

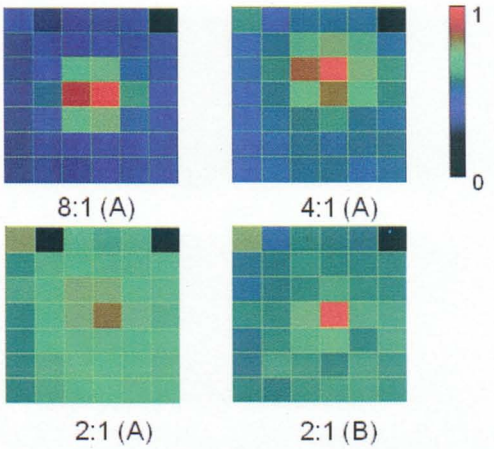

Figure 12. Images acquired from contrast tests with different activity ratios. For 2:1 ratio setting and position A, the actual ratio is less than 2:1, but the source was still resolved in the image.

5. CONCLUSIONS

We developed a gamma camera for imaging prostate cancer. Because of several advantages of CZT detectors over scintillation detectors and the development of highly integrated ASICs, the camera is compact and can function as a trans-rectal probe to image the prostate gland. Such a short working distance greatly improves the efficiency of detection and the spatial resolution. The prototype system demonstrated very promising imaging performance. The camera has high sensitivity, and it can detect low-contrast objects in a high background. Because of its high sensitivity, the camera potentially can work with a wide range of SPECT radiopharmaceuticals. Although the current prototype system does not have very high spatial resolution, it will be improved considerably after we have completed reducing the pixel pitch from 2.46 mm down to 1.6 mm or less. Our new results will be reported later.

6. ACKNOWLEDGEMENT

The authors would like to thank the U.S. Department of Energy's Office of Nonproliferation Research and Development (NA-22) as the principal sponsor funding the research on CZT detector development. The authors are also grateful to Hybridyne Imaging Technologies, Inc. for the funding support on the design, engineering and testing of the ProxiScan™ gamma camera.

REFERENCES

[1] www.cancer.org
[2] Per-Anders Abrahamsson and Martina Tinzl, "Do We Need PSA and Early Detection of Prostate Cancer?", European Urology Supplements 7, 2008, pp. 393-395.
[3] S. Jeschke, E. Schweigreiter and G. Janetschek, "Role of Imaging in Prostate Cancer: A Review", Imaging Decisions MRI, no. 13, 2010, pp. 68-87.
[4] Mohsen Beheshti, Werner Langsteger and Ignac Fogelman, "Prostate Cancer: Role of SPECT and PET in Imaging Bone Metastases", Semin. Nucl. Med. 39, 2009, pp. 396-407.
[5] www.radiologyinfo.org
[6] G. De Geronimo, A. Dragone, J. Grosholz, P. O'Connor and E. Vernon, "ASIC with Multiple Energy Discrimination for High-rate Photon Counting Applications", IEEE Trans. Nucl. Sci., vol. 54, issue 2, pp. 303-312, 2007.
[7] www.cypress.com
[8] "Performance measurements of scintillation cameras", NEMA Standards Publication No. NU 1, National Electrical Manufacturers Association, 2007.